2008

Nonmonotonicity in the quantum-classical transition: chaos induced by quantum effects

Arie Kapulkin

Arjendu K. Pattanayak
Carleton College

Nonmonotonicity in the Quantum-Classical Transition: Chaos Induced by Quantum Effects

Arie Kapulkin[1] and Arjendu K. Pattanayak[2]

[1]128 Rockwood Crescent, Thornhill, Ontario L4J 7W1 Canada

[2]Department of Physics and Astronomy, Carleton College, Northfield, Minnesota 55057

(Received 16 February 2007; published 11 August 2008)

The classical-quantum transition for chaotic systems is understood to be accompanied by the suppression of chaotic effects as the relative $\hbar$ is increased. We show evidence to the contrary in the behavior of the quantum trajectory dynamics of a dissipative quantum chaotic system, the double-well Duffing oscillator. The classical limit in the case considered has regular behavior, but as the effective $\hbar$ is increased we see chaotic behavior. This chaos then disappears deeper into the quantum regime, which means that the quantum-classical transition in this case is nonmonotonic in $\hbar$.

DOI: 10.1103/PhysRevLett.101.074101 PACS numbers: 05.45.Mt, 03.65.Sq

Open nonlinear quantum systems are critical in understanding the foundations of quantum behavior, particularly the transition from quantum to classical mechanics. For example, it has been argued that quantum systems decohere rapidly when the classical counterpart is chaotic, with the decoherence rate determined by the classical Lyapunov exponents of the system [1]. This applies to entanglement and fidelity as well [2–4], since decoherence amounts to entanglement with the environment.

A powerful way of studying open quantum systems is the quantum state diffusion (QSD) approach [5]. This enables the resolution of the paradox that in the absence of a QSD-like formulation, classical chaos cannot be recovered from quantum mechanics, indicating that the $\hbar \to 0$ limit is singular. Brun *et al.* [6] studied the convergence towards classical trajectories for a chaotic system with quantum Poincaré sections of the quantities $\langle \hat{x} \rangle$ and $\langle \hat{p} \rangle$. They showed that the classical chaotic attractor is recovered when the system parameters were such that $\hbar$ was small relative to the system's characteristic action. As the relative $\hbar$ increased, the attractor disappeared gradually, suggesting a persistence of chaos into the quantum region, consistent with later, more quantitative analyses [7,8]. Related work [9] studied a quantum system that is being continuously weakly measured, which leads to similar equations as those for QSD [10]. This also showed that chaos is recovered in the classical limit, and that it persists, albeit reduced, substantially into the quantum regime. Another related study [11] of coupled Duffing oscillators, showed that quantum effects, specifically entanglement, persist in a quantum system even when the system is classical enough to be chaotic.

The prevailing paradigm is that chaos is classical, and is suppressed quantum mechanically. Do quantum effects always decrease chaos, however? A closed Hamiltonian quantum system studied within a Gaussian wave packet (WP) approximation [12] manifested chaos absent classically. This has been understood to be an artifact of the approximation, since the full quantum system is not chaotic. Follow-up work with an open system [13] also manifested quantum chaos, but it is not clear if this was not due to the approximations made. However, contrary to the prevailing paradigm, the classical-to-quantum transition [14] for the δ-kicked rotor was shown to be nonmonotonic in the degree of diffusion, which is related to the degree of chaos in the problem.

In this Letter we show evidence of chaos being induced by quantum effects. Specifically, in a QSD system with a nonchaotic classical limit, as we increase the relative $\hbar$, chaos emerges, due to explicitly quantum effects (tunneling and zero-point energy) and as $\hbar$ is increased further, the chaos disappears. Although being reported for the first time, this intriguing result is arguably relatively common. Moreover, it shows that the quantum-classical transition for nonlinear systems is in general *not* monotonic in $\hbar$. The QSD evolution equation for a realization $|\psi\rangle$ of the system interacting with a Markovian environment is

$$|d\psi\rangle = -\frac{i}{\hbar}\hat{H}|\psi\rangle dt + \sum_j \Big(\langle \hat{L}_j^\dagger \rangle \hat{L}_j - \frac{1}{2}\hat{L}_j^\dagger \hat{L}_j - \frac{1}{2}\langle \hat{L}_j^\dagger \rangle \langle \hat{L}_j \rangle \Big) |\psi\rangle dt + \sum_j (\hat{L}_j - \langle L_j \rangle)|\psi\rangle d\xi_j, \quad (1)$$

where $\hat{H}$ is the Hamiltonian and the Lindblad operators $\hat{L}_j$ model coupling to an external environment. The density matrix is recovered as the ensemble mean M over different realizations as $\hat{\rho} = M|\psi\rangle\langle\psi|$ [5]. The $d\xi_j$ are independent normalized complex differential random variables satisfying $M(d\xi_j) = 0$; $M(d\xi_j d\xi_{j'}) = 0$; $M(d\xi_j d\xi_{j'}) = \delta_{jj'} dt$.

Consider specifically the classical driven dissipative Duffing oscillator

$$\ddot{x} + 2\Gamma\dot{x} + x^3 - x = g\cos(\Omega t), \quad (2)$$

for a particle of unit mass in a double-well potential, with dissipation Γ, and driving amplitude g and frequency Ω. Chaotic behavior obtains for certain ranges of Γ, g, Ω [15]. Chaos is found through Poincaré maps [obtained by recording (x, p) at time intervals of $2\pi/\Omega$]showing a strange attractor, or the behavior of the time series $x(t)$, or through a positive Lyapunov exponent. To quantize this problem [6,7] choose $\hat{H}$ and $\hat{L}$ for Eq. (1) as $\hat{H} = \hat{H}_D + \hat{H}_R + \hat{H}_{\text{ex}}$,

$$\hat{H}_D = \frac{1}{2m}\hat{p}^2 + \frac{m\omega_0^2}{4l^2}\hat{x}^4 - \frac{m\omega_0^2}{2}\hat{x}^2, \tag{3}$$

$$\hat{H}_R = \frac{\gamma}{2}(\hat{x}\,\hat{p} + \hat{p}\,\hat{x}), \tag{4}$$

$$\hat{H}_{\rm ex} = -gml\omega_0^2\hat{x}\cos(\omega t), \tag{5}$$

$$\hat{L} = \sqrt{\frac{m\omega_0\gamma}{\hbar}}\hat{x} + i\sqrt{\frac{\gamma}{m\omega_0\hbar}}\hat{p}. \tag{6}$$

After some redefinitions this reduces to the dimensionless Hamiltonian $\hat{H}_\beta$ and Lindblad operator $\hat{L}$ given by $\hat{H}_\beta = \hat{H}_D + \hat{H}_R + \hat{H}_{\rm ex}$ where $\hat{H}_D = \frac{1}{2}\hat{P}^2 + \frac{\beta^2}{4}\hat{Q}^4 - \frac{1}{2}\hat{Q}^2$, $\hat{H}_R = \frac{\Gamma}{2}(\hat{Q}\,\hat{P} + \hat{P}\,\hat{Q})$, $\hat{H}_{\rm ex} = -\frac{g}{\beta}\hat{Q}\cos(\Omega t)$, $\hat{L} = \sqrt{\Gamma}(\hat{Q} + i\hat{P})$, and $\Omega \equiv \omega/\omega_0$, $\Gamma \equiv \gamma/\omega_0$. The quantity $\beta^2 \equiv \frac{\hbar}{ml^2\omega_0}$ determines the relative system size, and the degree to which quantum effects influence the motion. Specifically [6,7] the limit $\beta \to 0$ yields the classical Eq. (2) while increasing β increases quantum corrections resulting in qualitatively different dynamics.

We have studied the quantum Duffing oscillator using the numerical QSD library [16]. All previous studies [6,7] changed β, with the parameters $\Gamma = 0.125$, $g = 0.3$ and $\Omega = 1.00$ held fixed so that they had the same chaotic classical limit [15]. We have studied 9 different families of quantum systems, each with a different classical limit, and examined 13 different values of β from essentially classical ($\beta = 0.01$) to the deep quantum regime ($\beta = 1.0$). We show six of these cases in the accompanying figures. Each simulation had the same initial state $|\psi(t=0)\rangle$—the coherent state $|\sqrt{2}(\langle\hat{Q}\rangle + i\langle\hat{P}\rangle) = (1.4 - 0.4i)\rangle$—and ran slightly over 500 periods of the external driving, yielding 500 post-transient points for the quantum Poincaré sections, shown for various β in Figs. 1(a)–1(c) as in [6,7]. We next consider the low-frequency power spectra, shown in Fig. 2, from the Fourier transforms $\tilde{X}(\varpi)$ of the time-series $\langle\hat{Q}(t)\rangle$; we show plots smoothed via a cubic spline in Fourier space to focus attention on the overall trend. We note both the broadband contributions of the noise in Eq. (1), and also an exponential increase in the power distribution in the low-frequency ($\varpi \ll \Omega$) limit. This low-frequency increase is characteristic of chaotic dynamics, and is absent in regular motion [17]. Now consider Figs. 3(a)–3(c), where we also show Poincaré sections, this time for $\Gamma = 0.3$, $g = 0.3$, and $\Omega = 1.00$. In marked contrast to the $\Gamma = 0.125$ situation, in this case we see the transition {regular → chaos → regular} as β is increased. That is, the system becomes chaotic as quantal effects are increased, and then becomes regular again in the deep quantal region, as also evident in the power spectra in Fig. 4.

To understand this, note that chaos occurs in such a system when trajectories sample the region near the unstable fixed point, and particularly the separatrix region, leading to interwell transitions. Thus, classically, a minimum amount of energy is needed for chaos. Compared to 1(a) the larger dissipation in 3(a) confines the system to one well and the external driving force is insufficient to over-

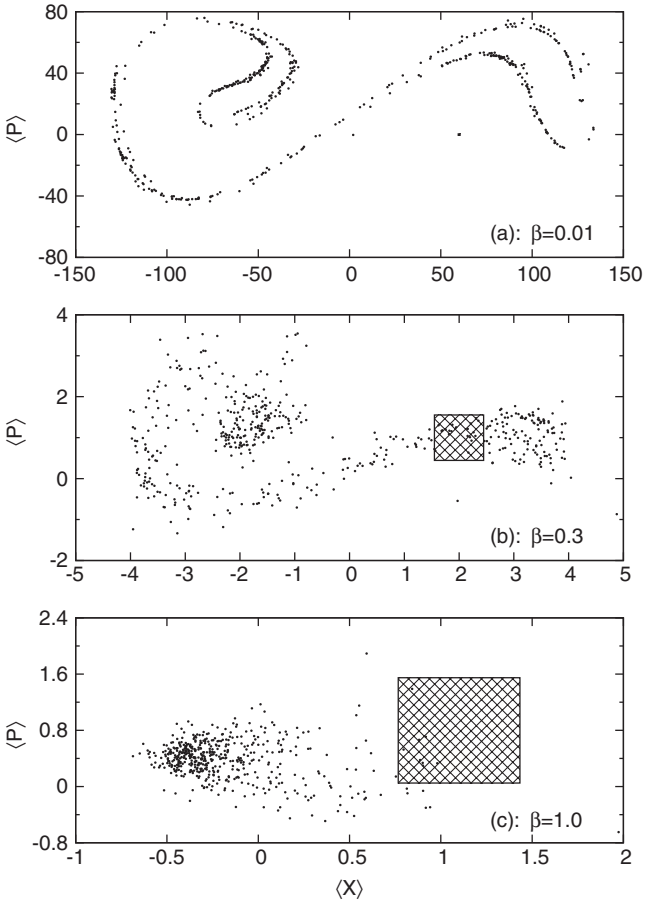

FIG. 1. Poincaré sections for $\Gamma = 0.125$, and $\beta = 0.01$, 0.3, 1.0 reading from top to bottom. The monotonic transition from classical chaos to quantum regularity is to be contrasted with the nonmonotonicity in Fig. 3. We also indicate the Planck cell with shaded squares of unit size representing $\hbar$.

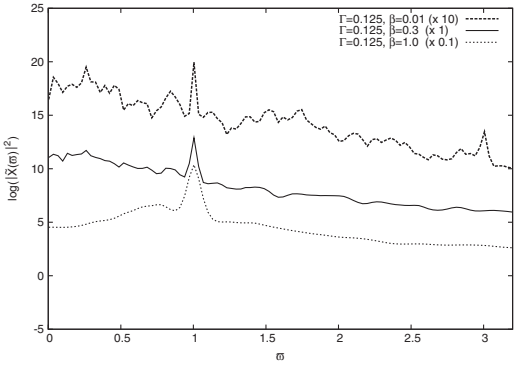

FIG. 2. Low-frequency power spectra for the 3 β values shown in Fig. 1, offset for visual clarity. We see the characteristic rise at low frequencies [17] for the chaotic cases, as well as the monotonicity of the transition with β.

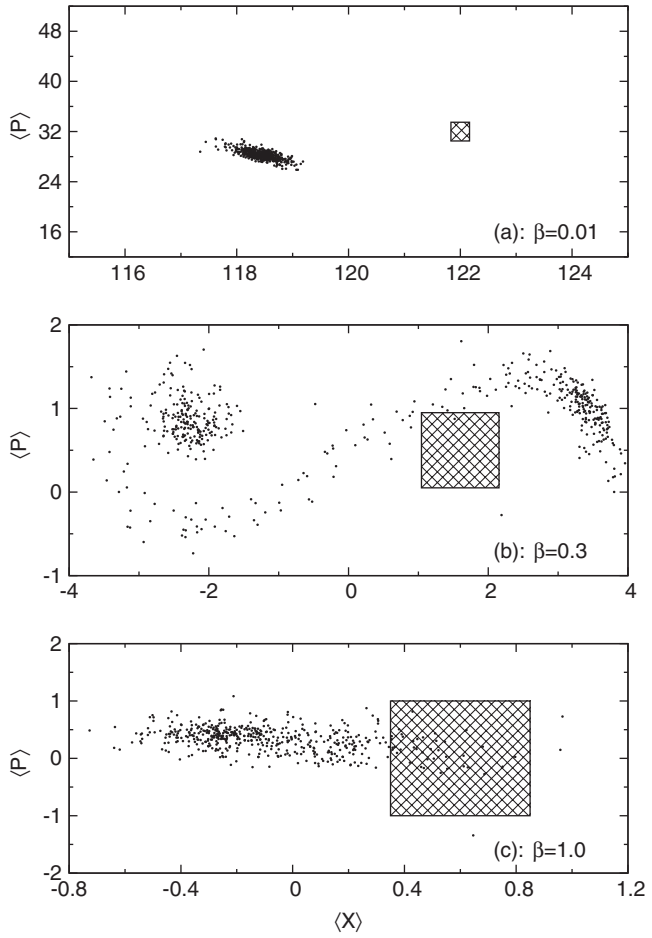

FIG. 3. Poincaré sections for $\Gamma = 0.3$, and $\beta = 0.01, 0.3, 1.0$ reading from top to bottom. The nonmonotonicity of {classical regularity → chaos → regularity} is to be contrasted with the monotonicity in Fig. 1.

come the potential barrier. Increasing β, however, increases the size of the WP moving in the classical potential, adding extra degrees of freedom (along with the "classical" centroid variables, there are now WP variances) and

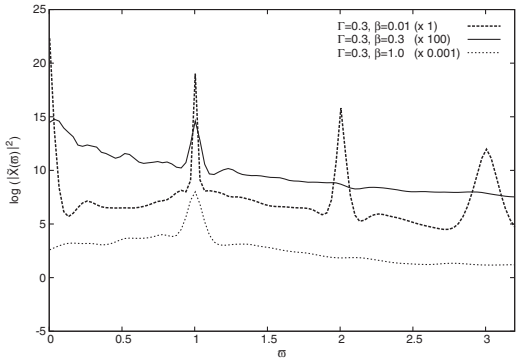

FIG. 4. Low-frequency power spectra for the 3 β values shown in Fig. 3, offset for visual clarity. We see the characteristic rise at low frequencies for the chaotic case, as well as the nonmonotonicity of the transition with β, to be contrasted with the monotonicity in Fig. 2.

changing the dynamics. It is useful to think of quantum dynamics as classical behavior in an effective potential, such that β controls the quantum effects in the effective potential [18]. The quantum corrections effectively raise the bottom of the well through added zero-point energy and also modify the well barrier, providing another route between the wells (tunneling).

These effects are readily apparent in time slices of the expectation values $\langle \hat{H} \rangle$, $\langle \hat{Q} \rangle$ shown in Figs. 5 and 6. In Figs. 5(a) and 6(a) we see classical behavior: transitions between wells only occur with positive energy. In Fig. 6(a), the energy is always negative, confining the system in one well. In Figs. 5(b) and 6(b) quantum effects are significant and the barrier is softened as the zero-point energy becomes significant and the potential barrier at $x = 0$ decreases. Now, transitions between wells occur, and even for negative energies, which we have indicated for 6(b) with a line at $t = 250.7$: this is quantum tunneling. Figures 5(c) and 6(c) show that in the deep quantum regime, the quantum effects are so large that the system effectively sees a single well potential leading to regular motion. The interplay between the localization due to the Lindblads and the

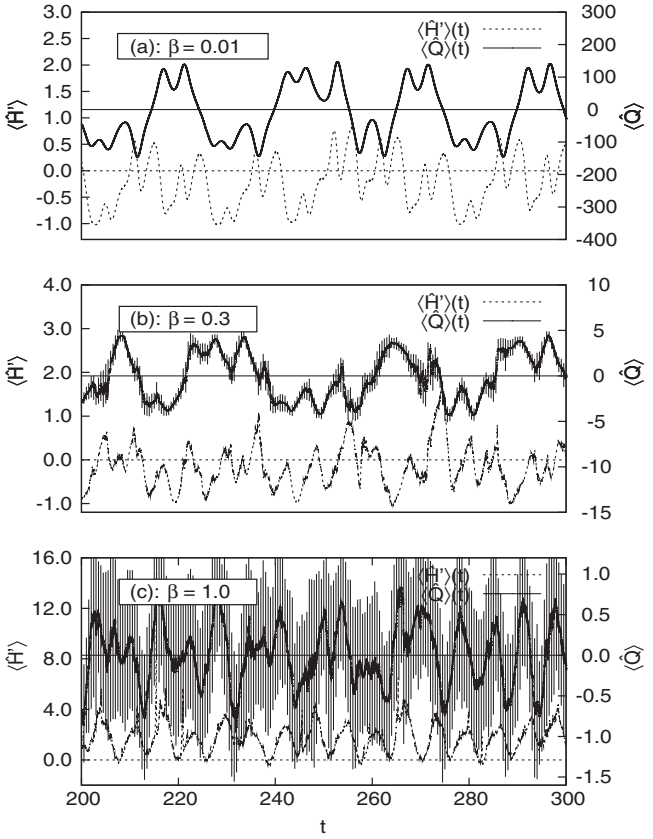

FIG. 5. Snapshots of the evolution of the expectation values of energy and position. The position curve also shows periodic "error bars," sampled to not swamp the graph, that measure wave packet width as $\sqrt{\langle (\hat{Q} - \langle Q \rangle)^2 \rangle}$. These are for $\Gamma = 0.125$, showing decreasing state localization, tunneling, and the effect of zero-point energy as β increases.

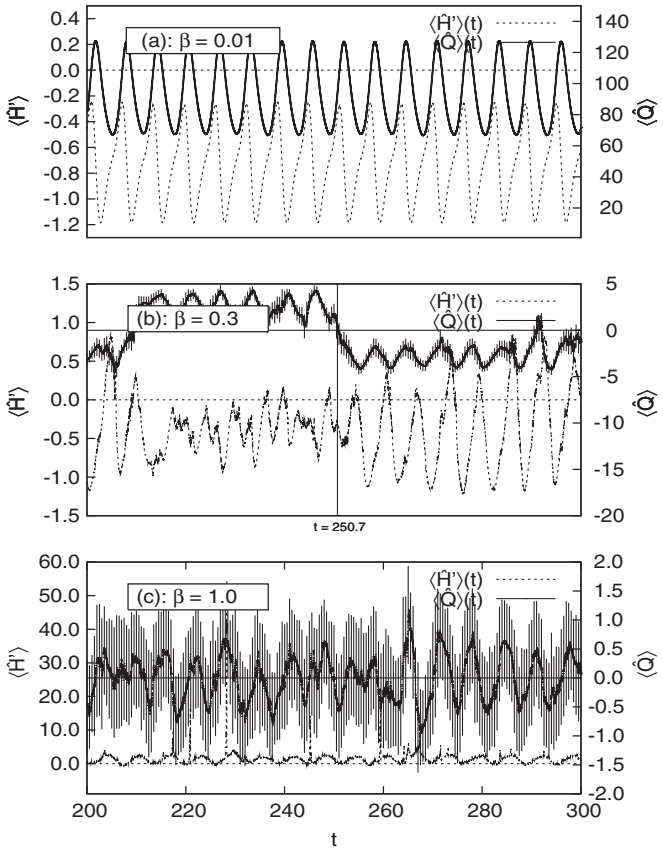

FIG. 6. As in Fig. 5 except that $\Gamma = 0.3$, showing clearly that tunneling and the zero-point energy lead to bistability and chaos in this case.

dynamics is also illuminating. For small β, the WP is sharply localized and essentially a point throughout, even when near the central barrier, as intuitive for ''near-classical'' dynamics. For the extreme quantal case, there is almost no localization. The case of most interest ($\beta = 0.3$) lies in between. Focusing on the interwell negative energy transitions (tunneling), there are no changes of shape as the WP transits across the barrier. Specifically, if visualized via the spread ($\sqrt{\langle(\langle\hat{Q} - \langle\hat{Q}\rangle)^2\rangle}$) as ''error-bars'' for the position ($\langle\hat{Q}\rangle$), we see the WP moving as a single coherent object between the two wells. Calculations of the time dependence of the probability of the particle being in a single well (not shown) are consistent with this picture.

Classically, changing β amounts to changing the units of measurement leaving the dynamics unchanged. Quantum dynamics *are* sensitive to the absolute size of the system in units of $\hbar$. This scale dependence, rather than a variation of the dynamical parameters of the system as in classical chaos, leads to chaotic behavior. Thus dynamics can be ''quantum'' (as evidenced by tunneling) and ''chaotic'' simultaneously, and specifically quantum effects *can* induce chaos. More broadly, quantum-classical transition can be nonmonotonic [14]. It is likely that this is a generic property of nonlinear systems described by Hilbert space trajectories.

A. K. P. gratefully acknowledges sabbatical leave support from Carleton College through the SIT, Wallin, and Class of 1949 Faculty Development funds. We thank Adam Steege and Christopher Amey for unreported calculations.

[1] W. H. Zurek and J. P. Paz, Phys. Rev. Lett. **72**, 2508 (1994).
[2] R. Jalabert and H. M. Pastawski, Phys. Rev. Lett. **86**, 2490 (2001).
[3] Ph. Jacquod, Phys. Rev. Lett. **92**, 150403 (2004); C. Petijean and Jacquod, *ibid.* **97**, 194103 (2006).
[4] P. A. Miller and S. Sarkar, Phys. Rev. E **60**, 1542 (1999); A. Lakshminarayan, *ibid.* **64**, 036207 (2001).
[5] I. C. Percival, *Quantum State Diffusion* (Cambridge University Press, Cambridge, U.K., 1998).
[6] T. A. Brun, I. C. Percival, and R. Schack, J. Phys. A **29**, 2077 (1996).
[7] Y. Ota and I. Ohba, Phys. Rev. E **71**, 015201(R) (2005).
[8] H. H. Adamyan, S. B. Manvelyan, and G. Yu. Kryuchkyan, Phys. Rev. E **64**, 046219 (2001).
[9] T. Bhattacharya, S. Habib, and K. Jacobs, Phys. Rev. Lett. **85**, 4852 (2000); S. Habib, K. Jacobs, and K. Shizume, *ibid.* **96**, 010403 (2006).
[10] See K. Jacobs and D. Steck, Contemp. Phys. **47**, 279 (2006).
[11] M. J. Everitt *et al.*, New J. Phys. **7**, 64 (2005).
[12] A. K. Pattanayak and W. C. Schieve, Phys. Rev. Lett. **72**, 2855 (1994).
[13] W. V. Liu and W. C. Schieve, Phys. Rev. Lett. **78**, 3278 (1997).
[14] T. Bhattacharya *et al.*, Phys. Rev. A **65**, 032115 (2002).
[15] J. Guckenheiner and P. Holmes, *Nonlinear Oscillators, Dynamical Systems and Bifurcations of Vector Fields* (Springer, Berlin, 1983).
[16] R. Schack, T. A. Brun, and I. C. Percival, J. Phys. A **28**, 5401 (1995); R. Schack and T. A. Brun, Comput. Phys. Commun. **102**, 210 (1997). This software package integrates Eq. (1), using a moving basis transformation, taking advantage of the solutions' localization in Hilbert space, with requisite algorithmic acceleration.
[17] See similar power spectra for quantum chaos in M. J. Everitt *et al.*, Phys. Rev. E **72**, 066209 (2005).
[18] D. O. Reale *et al.*, Phys. Rev. E **51**, 2925 (1995).